

# MITK Global Tractography - Application to the Corticospinal Tract

Peter F. Neher<sup>1</sup>, Bram Stieltjes<sup>2</sup>, Marco Reisert<sup>3</sup>, Ignaz Reicht<sup>1</sup>, Hans-Peter Meinzer<sup>1</sup>, and Klaus H. Fritzsche<sup>1,2,\*</sup>

<sup>1</sup> German Cancer Research Centre, Division of Medical and Biological Informatics,  
Im Neuenheimer Feld 280, 69120 Heidelberg, Germany

<sup>2</sup> German Cancer Research Center, Division of Radiology,  
Im Neuenheimer Feld 280, 69120 Heidelberg, Germany

<sup>3</sup> University Hospital Freiburg, Dept. of Radiology, Medical Physics,  
Breisacher Straße 60a, 79106 Freiburg, Germany

**Abstract.** In the DTI Tractography Challenge MICCAI 2011 different tractography algorithms compete in tracking the corticospinal tract. In this paper we present an implementation of the global tractography algorithm proposed by Reisert *et.al.* [1] using the open source Medical Imaging Interaction Toolkit (MITK) developed and maintained by the Division of Medical and Biological Informatics at the German Cancer Research Center (DKFZ). The MITK diffusion imaging application combines all the steps necessary for a successful tractography: preprocessing, reconstruction of the images, the actual tracking, live monitoring of intermediate results, postprocessing and visualization of the final tracking results.

**Keywords:** Global Tracking, Neuronal Tractography, Diffusion-weighted Imaging, Q-Ball Imaging, Diffusion Tensor Imaging

## 1 Introduction

Up to now, diffusion weighted imaging (DWI) is the only technique to noninvasively gain insight into the architecture of the human white matter pathways. Tractography algorithms try to explicitly estimate the underlying fiber pathways from the given voxelwise information.

There exists a wide variety of different tractography algorithms that can be roughly divided into the two subgroups of local and global methods. Local methods try to reconstruct one fiber at a time by following the voxelwise information and successively adding segments to the fiber. Fibers can either be generated following a model-based or a model-free approach. While local methods are known to be performant, they often struggle with image artifacts or complex fiber configurations like crossings or kissings. Global methods try to reconstruct all fibers simultaneously, searching for a global optimum. While computationally much

---

\* Corresponding author. E-mail address: k.fritzsche@dkfz-heidelberg.de.

more challenging, global methods promise more robust results. This work presents the integration of the successful [2] and also computationally efficient global approach proposed by Reisert *et.al.* [1] within the Medical Imaging Interaction Toolkit (MITK) developed at the German Cancer Research Center (DKFZ) and its application to reconstruct the corticospinal tract. MITK is a free open-source software system for development of interactive medical image processing software [3]. The diffusion imaging application is available on [www.mitk.org](http://www.mitk.org) and we are in the process of publishing it open source. This paper describes the processing pipeline that was applied to the datasets provided by the organizers of the DTI Tractography Challenge MICCAI 2011 to obtain tractography results of the corticospinal tract (CST).

## 2 Materials and Methods

Three steps were performed in order to obtain the desired reconstruction of the CST. The first step includes preprocessing and generation of additional information like mask images. The second step consists of the actual tractography and the third step describes the extraction of the corticospinal tract from the whole brain tracking result. The process is illustrated in Fig. 1.

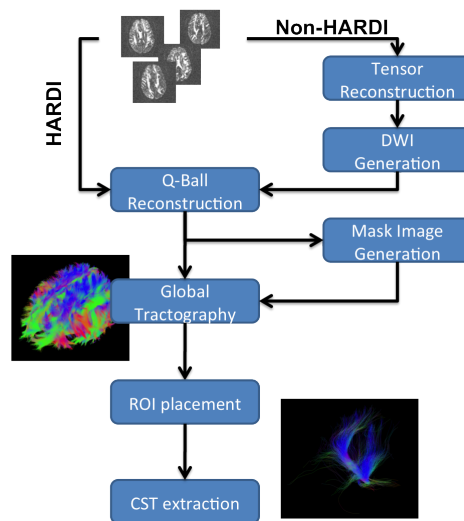


**Fig. 1.** Flowchart of the processing steps from DWI images to the extracted CST.

### 2.1 DWI Processing Pipeline

Depending on the type of acquisition, different reconstruction methods for the DWI can be chosen. Our tractography algorithm expects ODFs as input data.

If the DWI is already captured using a high angular resolution diffusion imaging (HARDI) sequence, the Q-Ball reconstruction can be performed directly. Otherwise a standard tensor reconstruction is applied and a new DWI image with high angular resolution is estimated from the tensor image. The resulting DWI image can then be processed via Q-Ball reconstruction.

In this work, the supplied DTI datasets were used directly instead of a reconstruction of the tensor data from the provided DWI datasets. There are several different Q-Ball reconstruction methods available in MITK like a numerical reconstruction (Tuch *et.al.* [4]) or a spherical harmonics reconstruction with solid angle consideration (Aganj *et.al.* [5]). In this work we used a basic spherical harmonics reconstruction as proposed by Descoteaux *et.al.* [6]. The applied tracking approach does not need a mask image to yield accurate tracking results, but by limiting the search space with a binary brain mask, the process can be accelerated considerably. The mask image was generated by a simple thresholding of the GFA image generated from the reconstructed Q-Ball image. The thus produced Q-Ball and mask images are used as input for the tracking algorithm.

## 2.2 Global Tractography

The basic idea of the global tractography algorithm [1] is to fit a model  $M$ , consisting of directed points (particles) and connections between the particles, to the image data  $D$  by minimizing two energy terms.

The first energy, the so called external energy  $E_{ext}$ , measures the distance from the artificial signal  $\rho_M$  computed from the current model configuration to the original image data, i.e. the external energy ensures that  $M$  is able to explain the signal in the best possible way. The external energy is computed as

$$E_{ext}(M, D) = \lambda_{ext} \|\rho_M - D\|_{L_2(\mathbb{R}^3 \times S_2)}^2, \quad (1)$$

where  $\lambda_{ext}$  is a weighting factor controlling the balance between external and internal energy.

The second energy, the internal energy  $E_{int}$ , applies certain constraints to the model itself. It is designed to enforce long and straight fibers. By minimizing  $E_{int}$  the model is shaped in a way that is consistent with structural knowledge about neuronal fibers. Each particle can connect to another particle with one of its endpoints. A chain of connected particles represents a fiber. The connection potential between two particles is small if the endpoints of two connected particles lie close together and point in the same direction.

To optimize the model, the whole problem is formulated as a maximization of the a-posteriori probability of the model  $M$  given the image data  $D$ :

$$P(M|D) = \exp(-E_{int}(M)/T - E_{ext}(M, D)/T), \quad (2)$$

$P(M|D)$  is maximized via the introduction of random change proposals with a certain probability  $p_{prop}$  into the model  $M$ . The resulting model configuration  $M'$  is afterwards accepted or rejected according to a certain ratio calculated from  $P(M'|D)$  and  $P(M|D)$ . By successively reducing the temperature  $T$  it becomes

more and more likely to converge to a steady and optimal configuration of the model. For more details regarding the algorithm, please refer to [1].

To increase the number of detected fibers and to account for the statistical nature of the process, each image was tracked four times with  $10^8$  iterations for each image and the results were combined afterwards.

### 2.3 Extraction of the Corticospinal Tract

The tractography approach described in the previous subsection yields a whole brain tracking result. To extract the CST from the whole brain result seven ROIs were placed manually. The first ROI ( $R1$ ) is placed in a transversal slice on the brain stem at about the height of the Pons, while catching both strands of the corticospinal tract and avoiding the Superior Cerebellar Peduncle and the Medial Lemniscus. The second and third ROI ( $R2$ ,  $R3$ ) are placed on the posterior limb in the internal capsule of the respective hemisphere to catch the fibers spreading out to form the Corona Radiata. The fourth ROI ( $R4$ ) is placed sagittally between the two hemisphere to catch and erase fibers crossing the Corpus Callosum. The three ROIs  $R5 - R7$  are placed left, right and behind the lower part of the CST to erase the remaining fibers of the Superior Cerebellar Peduncle and the Medial Lemniscus. The ROIs were placed similarly for all 22 images. A schematic ROI placement of  $R1 - R6$  is depicted in Fig. 2 ( $R7$  was omitted in this figure due to clarity issues). The ROIs are combined via logical operations to extract or avoid fibers respectively in the following manner:

$$R = R1 \wedge (R2 \vee R3) \wedge \neg(R4 \vee R5 \vee R6 \vee R7) \quad (3)$$

All fibers that do not pass through the composite ROI  $R$  are removed.

## 3 Results

The method described in chapter 2 was applied to all provided 22 diffusion tensor images obtained from four different probands. Ten images each were obtained from two healthy subjects and one image from two surgical cases respectively. In all images the corticospinal tract was detected successfully. Figure 3 shows the sagittal and coronal tracking results of all 22 images. Fig. 4 shows the whole brain tracking result of the patient 1 dataset as well as the according extracted CST and ROIs used for the extraction in four different views.

## 4 Discussion and Conclusion

In this paper we presented tracking results of the CST using MITK global tractography. The CST was successfully tracked in the diffusion weighted images supplied by the Organizers of the DTI Tractography Challenge MICCAI 2011. Surprisingly some branches of the corona radiata of the CST were detected more satisfying in the healthy subject datasets which are of much lower resolution

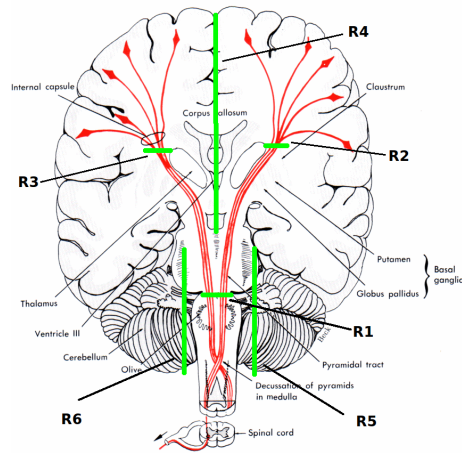


**Fig. 2.** Schematic placement of the ROIs (green) used to extract the corticospinal tract from the whole brain tracking (R7 omitted). Image adapted from [7]

and quality than the two neurosurgical datasets. A qualitative evaluation of the according region lead to the conclusion that the image data of the two neurosurgical subjects in fact does not supply the information needed to reconstruct the according fiber tracts. The issue is illustrated in Fig. 5.

## References

1. Reisert, M., Mader, I., Anastasopoulos, C., Weigel, M., Schnell, S., Kiselev, V.: Global fiber reconstruction becomes practical. *Neuroimage* **54** (2011) 955–962
2. Fillard, P., Descoteaux, M., Goh, A., Gouttard, S., Jeurissen, B., Malcolm, J., Ramirez-Manzanares, A., Reisert, M., Sakaie, K., Tensaouti, F., Yo, T., Mangin, J.F., Poupon, C.: Quantitative evaluation of 10 tractography algorithms on a realistic diffusion MR phantom. *Neuroimage* **56**(1) (2011) 220–234
3. MITK.org: The Medical Imaging Interaction Toolkit MITK. [Online]. Available: <http://www.mitk.org>. [Accessed: April 12, 2011] (2005)
4. Tuch, D.S.: Q-Ball Imaging. *Magnetic Resonance in Medicine* **52** (2004) 1358–1372
5. Aganj, I., Lenglet, C., Sapiro, G.: Odf reconstruction in q-ball imaging with solid angle consideration. In: *Sixth IEEE International Symposium on Biomedical Imaging*. (2009)
6. Descoteaux, M., Angelino, E., Fitzgibbons, S., Deriche, R.: Regularized, Fast, and Robust Analytical Q-Ball Imaging. *Magnetic Resonance in Medicine* **58** (2007) 497510
7. arthursclipart.org: Corticospinal Tract. ([Online]. Available: <http://www.arthursclipart.org> [Accessed: June 7, 2011])

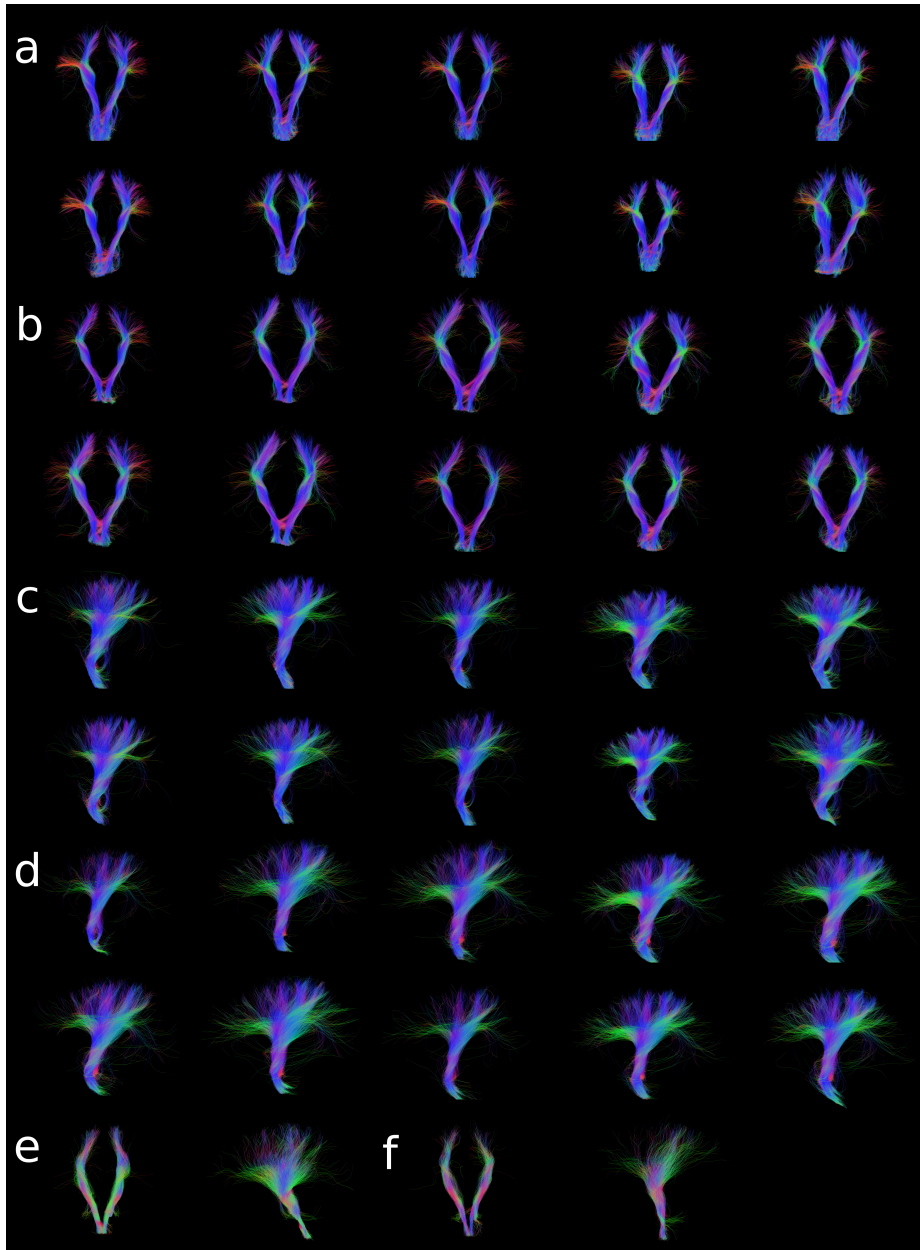


**Fig. 3.** (a) CST tracking of healthy subject 1 (coronal view) (b) CST tracking of healthy subject 2 (coronal view) (c) CST tracking of healthy subject 1 (sagittal view) (d) CST tracking of healthy subject 2 (sagittal view) (e) CST tracking of patient 1 (coronal and sagittal view) (f) CST tracking of patient 2 (coronal and sagittal view).

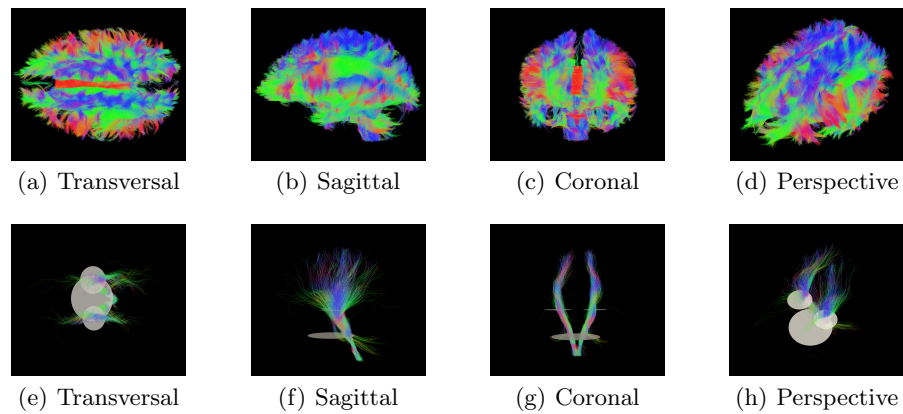


**Fig. 4.** a-d: Whole brain tractography result of the patient 1 dataset. e-h: CST tracts including ROIs used for the extraction (negative ROIs omitted).

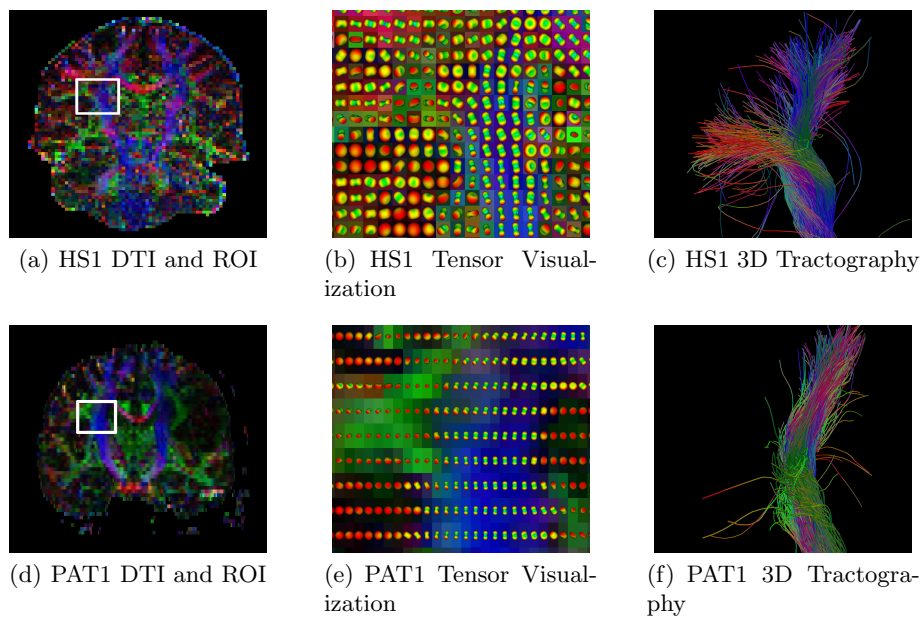


**Fig. 5.** Comparison between healthy subject 1 (upper row) and patient 1 (lower row) in the branching regions of the corona radiata. The left column (image (a) and (d)) show the coronal view of both images with a ROI marked as white rectangle. Image (b) and (e) depict the tensor visualization of the according ROI and the rightmost column (image (c) and (f)) shows the respective 3D visualization of the tracking result. The neurosurgical dataset does not seem to supply the information needed for a successful tracking of the branching.